FINAL

DETERMINING WIND SPEED AND DIRECTION WITH OCEAN REFLECTED GPS SIGNALS *

Cinzia Zuffada
Jet Propulsion Laboratory
California Institute of Technology
Pasadena, CA 91109-8099

Tanos Elfouhaily
The Johns Hopkins University
Applied Physics Laboratory
Laurel, MD 20723-6099

ABSTRACT

The power received by a GPS receiver located on an airplane flying over the ocean and collecting the GPS signal reflected off the surface is estimated for varying wind speed and wind direction, platform altitude, satellite elevation angle, and receiver integration time. By accounting for the wind-induced anisotropy on the surface, it is shown that the trailing edges of computed waveforms change with both wind speed and direction. Different wind directions cause substantial differences in the waveforms, particularly for low-elevation reflections. While this feature allows the retrieval of both modulus and direction it also creates an ambiguity if one tries to solve for modulus only, while neglecting direction. An effective retrieval scheme must include observations from a variety of satellites, possibly including high elevation ones, whose corresponding waveforms are insensitive to direction.

1.0 INTRODUCTION

The possibility of using the GPS signal reflected off the ocean surface as a means for remote sensing of the ocean has generated considerable attention in the past few years. In fact, the availability of the existing constellation of transmitters and the continuous progress in the GPS receiver technology indicate that GPS-based remote sensing could be relatively inexpensive and yet provide global, dense, and frequent coverage of the Earth. Two specific applications which are currently being investigated are sea surface altimetry [*Martin-Neira*, 1993, *Picardi* et al., 1998, *Hajj* et al., 1999] and scatterometry [*Zavorotny* et al., 1999, *Bin* et al., 1999, *Garrison* et al., 1999]; this paper addresses the latter.

The first theoretical description of the GPS reflected waveform measured by a receiver on a moving platform, namely an airplane, appeared in [*Zavorotny* et al., 1999]. That work was based on a geometric optics (GO) approximation of a simplified Kirchhoff's scattering theory and utilized the model for the wind-driven ocean wave spectrum developed in [*Elfouhaily* et al., 1997]. According to this theory, the effect of the wind on the scattering cross section coefficient is quantified by the surface slope variances, which depend on wind direction in addition to wind speed. The authors calculate the received power waveform corresponding to different wind speeds. They also discuss the behavior of the trailing edge at typical airplane altitudes (10 km in their example). They conclude that the sensitivity of the trailing edge to wind direction is

* Presented at the Sixth International Conference on Remote Sensing for Marine and Coastal Environments, Charleston, South Carolina, 1-3 May 2000.

manifested only at late time delays, so it has little practical utility because the power level is very low. Hence, they advocate a unique correspondence between wind speed and rate of decay of the trailing edge, which can be used as a detector of wind speed in a retrieval algorithm.

In this paper, using the same spectrum and a similar (although not exactly the same) scattering theory, we investigate the sensitivity on the trailing edge of the waveform to the direction of the wind relative to the bistatic reflection geometry, for varying airplane altitudes and elevation angles. We attribute the differences to the fact that the area on the ocean, that contributes to the received power (elliptical annulus), does not grow isotropically as a function of time but rather stresses preferential geometric directions. Additionally, a GPS receiver performs an integration (cross correlation) of the signal over a time commensurate with the coherence of the process being observed, in this case the scattering from the ocean. As will become clear in the paper, this operation amounts to spatially filtering the contributions to the waveform in a manner controlled by the orientation of the receiver velocity vector relative to the plane of reflection and the integration time. This amplifies the difference in the trailing edge of waveforms corresponding to the same wind speed but different wind directions. When this operation is accounted for and realistic integration times are used, one can see that the trailing edges corresponding to the same wind speed but different wind directions are significantly different at earlier times, thus allowing to detect both speed and direction of winds.

2.0 GPS REFLECTED WAVEFORM

A thorough derivation of the received power waveform is contained in [*Zavorotny* et al., 1999]. Furthermore, in [*Ha*jj et al., 1999] the additional effect of the statistical distribution of specular reflection points on the leading edge of the waveform is discussed, of particular relevance when altimetry is considered. It is obtained

$$P(\tau) = A \int \frac{\Lambda_m^2(\tau - (R_1(\xi) + R_2(\xi))/c)}{R_1^2(\xi) R_2^2(\xi)} \; \sigma_0(U_{10},(\xi)) \;\; F(\Delta f(\xi)) \;\; d^2\xi \qquad (1)$$

where τ is the observation time measured relative to the arrival of the contribution from the specular reflection point, Δ_m is the modified correlator function accounting for the statistical distribution of heights [*Hajj* et al., 1999], σ_0 is the scattering cross section coefficient and depends on the probability density of surface slopes (and hence wind speed at a height of 10 m, U_{10}) in a manner described in [*Zavorotny* et al., 1999], F(.) is the spatial filtering function associated with the receiver integration time, and the integral is performed over the ocean surface, whose generic point is represented by the vector ξ with origin at the specular reflection point. The constant A is a scaling factor which represents the incident GPS power and the receiving antenna gain assumed constant. It has already been pointed out that the area contributing to the power received at a given time is a thin elliptical annulus, moving outwardly as time increases. The ellipses are generated by the intersection of the equirange spheroid with receiver and transmitter at its foci and the tangent plane to the earth at the specular reflection point. For convenience, ranges are measured relative to a minimum range, corresponding to the specular reflection point, and are expressed as integers of the chip length. The GPS chip rate is the frequency of probable occurrence of a code transition, and is 1.023 MHz for C/A code. The corresponding length is nothing but the ratio of the speed of light and the chip rate (~300m). To understand the effect of the wind direction on the received waveform it is useful to describe first the behavior in the growth of the annulus.

2.1 SPATIAL ASYMMETRY OF BISTATIC GEOMETRY

The distribution of the iso-range ellipses for ranges up to 10 code chips (in excess of the minimum range) are illustrated in Fig 1 for the situation of a receiver at 5 Km altitude and for two satellites elevations, 30° and 70°, respectively.

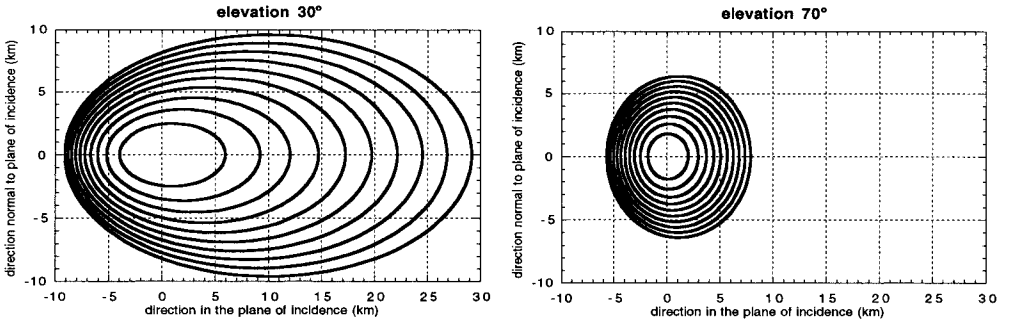

Figure 1. Iso-range ellipses for airplane altitude of 5 km and two different elevations.

Note the highly asymmetric behavior of the iso-range contours at low elevation (30°), as expressed by the ratio of semi-major/semi-minor ellipse axes, compared with the situation at high elevation (70°), resulting in a high eccentricity of 0.9. By introducing the plane of incidence as that containing the receiver, transmitter and reflection point, we can see that it is also the plane of symmetry of the ellipses, which contains the major axes. The plane of Fig. 1 is thus perpendicular to the plane of incidence. The centroid of the ellipses moves along the direction of the major axes towards the transmitter by as much as 10 km for the case of satellite at low elevation. As a consequence, the annuli thickness can be 8 times higher in the direction towards the transmitter than that towards the receiver for the case of low elevation. This asymmetry indicates that the ocean surface, which is sensed in the reflection process, extends preferentially along the direction in the plane of incidence towards the transmitter. Even though the receiver performs an azimuthal integration while constructing the waveforms, most of the contribution is coming effectively from only one direction defined by the major axis of the iso-range ellipses. This feature along with an additional one related to the Doppler spreading as explained below will be the cornerstone for the wind vector retrieval.

2.2 SCATTERING BEHAVIOR

Let us consider the behavior of the scattering cross section coefficient, as a function of wind speed and wind direction. The spatial behavior is dominated by the exponentially decaying term in the probability density of slopes [*Zavorotny* et al., 1999]. Specifically, the rate of decay varies azimuthally on the ocean surface relative to the direction of the wind. Since the mean square slope is highest along the upwind direction and lowest along the crosswind direction, the exponential decay will behave in the opposite sense. Consequently, the decay is lowest in the upwind direction. Because of the asymmetric spatial sampling of the bistatic geometry, we expect that the trailing edge of the received power waveform will be the highest when the wind blows in the direction in the plane of incidence, and lowest when the wind blows in the direction

perpendicular to the plane of incidence, and these differences will be more pronounced the lower the satellite elevation. Based on the geometric symmetry and that of the probability density of

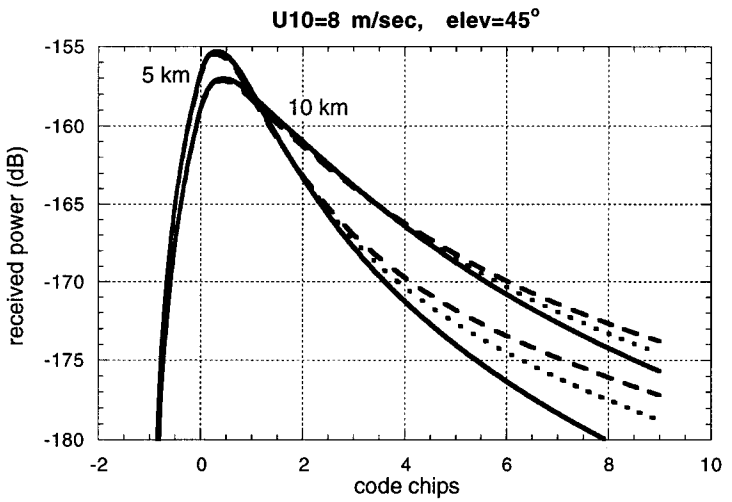

Figure 2. The continuous line indicates wind along the ellipses minor axis, the broken line indicates wind along the ellipses major axis and the dotted line indicatewind in between the two directions.

slopes, one can expect an ambiguity in resolving the wind direction with respect to the plane of symmetry, namely the plane of incidence. Hence, any two directions of the plane of Fig. 1 making opposite angles relative to the ellipses major axes give rise to the same predicted waveforms. Additionally, for any given direction it is not possible to identify the orientation to ±180° of the wind.

3.0 PREDICTED WAVEFORMS

3.1 THEORETICAL LIMIT

Simulations were performed for two airplane altitudes, namely 5 km and 10 km, at an elevation angle of 45°, and first assuming that the receiver integrates for a very short time. In both cases the wind speed was 8 m/sec. This result is a theoretical upper limit for the predicted signal level, a more realistic case is considered later. The results are presented in Fig. 2. The figure indicates a better sensitivity to wind direction at the lower airplane height, due to the higher asymmetry in the iso-range ellipses and the more limited extent of the glistening zone. In both cases the areas corresponding to the first few chips do not contribute to differences in the trailing edge of the waveform. The results illustrated above are encouraging but indicate that to detect the spread in trailing edges considerable equipment sensitivity is needed. However, we need to consider realistic receiver integration times and examine the spatial filtering effects introduced on the received waveform to fully understand its impact on the ability to detect wind direction.

3.2 RECEIVER INTEGRATION TIME

When processing the received data stream, a coherent integration time is chosen during which cross correlations between the data and a code replica, or expected signal, are performed over a range of values for the delay and the Doppler to maximize the operation output. At the end

a time series, analogous to the waveforms presented in Fig. 2, is produced corresponding to the optimal value of Doppler and delay. The Doppler value is sometimes referred to as the receiver compensation Doppler. Since the Doppler of the points on the ocean varies (iso-Doppler lines are hyperbolae), the compensation process will match the value very well at some points, namely along the correct iso-Doppler, and less so away from them, resulting in a reduction in the available signal to noise ratio. Fixing the integration time T_i is equivalent to setting a bandwidth in the receiver, meaning that oscillations (Doppler shifts) higher than the threshold set by the reciprocal of the integration time, are not resolved. This process amounts to a spatial filtering, described in Eq. 1 by the term $F(\Delta f)=[\sin(2\pi*\Delta f*T_i)/(2\pi*\Delta f*T_i)]^2$. The frequency bandwith Δf indicates the difference between the compensation value, normally the Doppler at the specular reflection point, and that of any given point on the ocean surface nearby.

Consequently, the coherent integration time is dictated by the process being observed. During the coherent integration it is assumed that the 'active' surface being observed does not change practically and that its field contributions to the received signal have phase coherence [*Born and Wolf*, 1980]. An upper bound is given by

$$T_i = \frac{Dist * \lambda}{diam * vel} \tag{2}$$

where *Dist* indicates the distance between the 'active' surface and the receiver, λ is the wavelength of the GPS carrier (~ 19 cm for L1, ~ 25 cm for L2), *diam* is the equivalent diameter of the 'active' surface and *vel* is the velocity of the receiver. For the case of a receiver at 10 km with a velocity in the range 100-200 m/sec, we obtain integration times of order 5-10 msec corresponding to areas of the first few chips. Having established a realistic value for the integration time, let us examine the corresponding Doppler filtered waveforms.

3.3 DOPPLER FILTERED WAVEFORMS

Calculations were performed for the case of airplane altitude of 10 km, and satellite at 45° elevation. The wind speed was assumed at 8 m/sec and blowing either along the major or minor ellipse axis. The velocity of the receiver was assumed at 200 m/sec with a velocity vector either in the plane of incidence or perpendicular to it. The time of coherent integration was taken to be 5 msec. The received power waveforms are illustrated in Fig. 3.

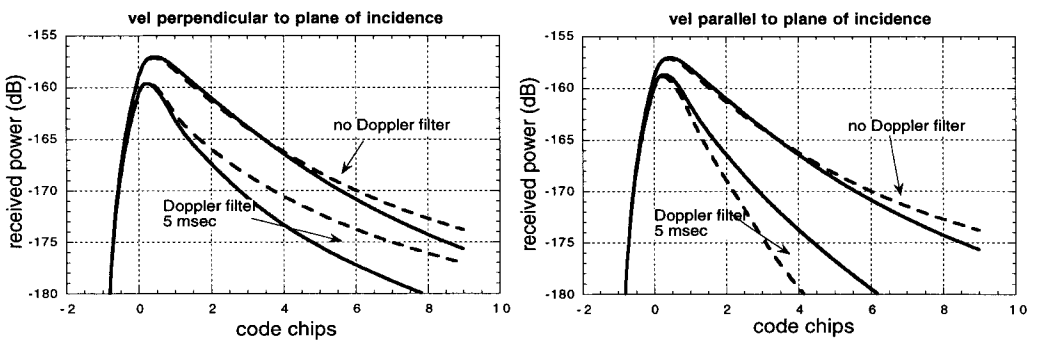

Figure 3. The continuous line indicates wind along the ellipses minor axis, the broken line indicates wind along the ellipses major axis.

Figure 3 clearly shows a noticeable separation in the trailing edge of the waveforms corresponding to the same wind speed but different direction, beginning after only the first chip. The case of velocity perpendicular to the plane of incidence is particularly promising because the trailing edge lasts longer, therefore possibly allowing for an easier detection. Indeed, when the realistic Doppler filtering operation performed by the receiver is properly accounted for, the sensitivity to wind direction is greatly enhanced. Similar results hold for other airplane altitudes, with the understanding that integration times depend on receiver velocity and altitude and will have to be adapted properly.

3.4 AMBIGUITY IN WIND SPEED/DIRECTION DETERMINATION

Let's examine now the expected waveforms for a variety of wind speeds and for different wind directions. We chose the same geometric and receiver parameters used for the study of subsection 3.3 and investigated the range 4-12 m/sec wind speed. The case of the velocity in the plane perpendicular to the plane of incidence was considered. The results are illustrated in Fig. 4.

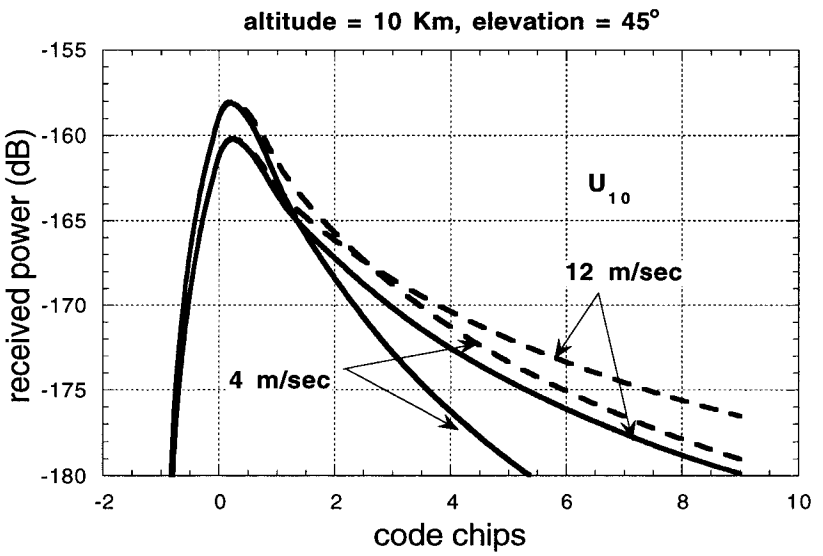

Figure 4. Continuous lines indicate wind along the ellipses minor axis, the broken lines indicate wind along the ellipses major axis

Figure 4 illustrates the spread of trailing edges corresponding to two different wind speeds, any intermediate value of wind speed would have a spread contained in the envelope between the highest and lowest curve of the figure. It is immediately observed that changes in trailing edges can be caused by variations in either wind speed or wind direction and this creates an ambiguity in the retrieval process. To overcome this ambiguity, waveforms from multiple satellites at different elevation must be considered, including high elevation ones, which are less sensitive to wind direction and can provide a strong constraint on the wind speed solution. To resolve the ambiguity in direction and orientation, two measurements coming from low elevation satellites having azimuthal separation of less than 90° are needed. In this case their corresponding iso-range ellipses form an angle between their main axes equal to the satellite azimuthal separation. Hence, while for each geometry there are four possible directions/orientations which

correspond to a given waveform, there is a unique wind direction/orientation which is common to both geometries.

4.0 CONCLUSIONS

The paper discusses how the wind speed and direction affect the GPS ocean reflected waveform and identifies strategies for retrieval of these parameters. The crucial role is played by the receiver integration time which, by introducing a spatial filtering, gives rise to different trailing edges of the waveform corresponding to different directions but the same wind modulus. In particular, observations from both high elevation and low elevation satellites must be available; the former to determine speed and the latter to determine direction. It is not possible to solve for speed alone, particularly when relying on measurements corresponding to low elevation satellites. By contrast, these very measurements are required to determine direction. In particular, measurements from two low elevation satellites separated in azimuth by less than 90° are sufficient to resolve the ambiguity in determining the direction of the wind.

5.0 ACKNOWLEDGEMENTS

The research described in this paper was carried out by the Jet Propulsion Laboratory, California Institute of Technology, under a contract with the National Aeronautics and Space Administration.

6.0 REFERENCES

Born M. and E. Wolf, *Principles of Optics*, Pergamon Press, Oxford, pp. 510-514, 1980.

Elfouhaily T., B. Chapron, K. Katsaros and D. Vandemark, " A unified directional spectrum for long and short wind-driven waves," *J. Geophys. Res.*, vol. 102, pp. 15,781-15,796, 1997.

Garrison J.L., A. Komjathy, V. Zavorotny and S.J. Katzberg, " Wind speed measurement from bistatically scattered GPS signals, submitted to *IEEE Transactions on Geoscience and Remote Sensing,* 1999.

Hajj G., C. Zuffada and J.B. Thomas, "Theoretical Description of a Bistatic System for Ocean Altimetry Using the GPS Signal," submitted to *IEEE Transactions on Geoscience and Remote Sensing,* 1999.

Lin B., S.J. Katzberg, J.L. Garrison and B.A. Wielicki, " Relationship between GPS signals reflected from sea surfaces and surface winds: Modeling results and comparisons with aircraft measurements," *J. Geophys. Res.*, Vol. 104, n. C9, pp. 20,713-20,727, Sept. 1999.

Martin-Neira M., "A passive reflectometry and interferometry system (PARIS): application to ocean altimetry," *ESA Journal*, vol. 17, pp. 331-355, 1993.

Picardi G., R. Seu, S. G. Sorge and M. Martin-Neira, " Bistatic model of ocean scattering", *IEEE Transactions on antennas and propagation,* Vol. 46, n. 10, pp. 1531-1541, Oct. 98.

Zavorotny V.U., and A. G. Voronovich, " Scattering of GPS signals from the ocean with wind remote sensing application," accepted for publication in *IEEE Transactions on Geoscience and Remote Sensing*, 1999.